

## Low-Temperature Anharmonicity in FeCl<sub>2</sub>\*

D. P. JOHNSON† AND J. G. DASH

University of Washington, Seattle, Washington 98105

(Received 2 April 1968)

Mössbauer spectra of Fe<sup>57</sup> in thin anhydrous ferrous chloride powdered absorbers have been investigated at several temperatures between 300 and 10°K. The quadrupole splitting, velocity shift, and Mössbauer fraction have been determined. The Mössbauer fraction of FeCl<sub>2</sub> shows an anomalously weak temperature dependence which cannot be explained by any harmonic model for the interatomic forces or by the usual high-temperature anharmonicity. This anomalous behavior implies a low-temperature anharmonicity which is qualitatively explained in terms of the relative sizes of the ions involved. The interpretation is consistent with the finding of essentially harmonic behavior for FeF<sub>2</sub>. The results of our reexamination of other Mössbauer *f* studies are also consistent with these size arguments.

### I. INTRODUCTION

THE Mössbauer effect can be used with particular advantage to measure the mean-square displacement (MSD) and mean-square velocity (MSV) of suitable ions in crystals. These two basic characteristics of the ionic motions provide sensitive gauges of the atomic-force constants and the phonon-frequency distribution. Although other techniques, such as inelastic neutron scattering, may yield more detailed information on the phonon-frequency distribution, the Mössbauer effect can give accurate measurements of certain integral moments of the frequency distribution, which are sensitive tests of harmonicity.

In the experiments described in this paper, the MSD and MSV of ferrous ions in FeCl<sub>2</sub> were measured with sufficient accuracy to provide a more stringent test of harmonicity than has usually been applied. Analysis of the results indicate that the harmonic approximation is unsuitable for this material. Reexamination of previously reported work suggest a similar breakdown of the harmonic approximation for other materials.

Since in a general harmonic crystal there is a force constant between one atom and every other atom in the crystal, it might be expected *a priori* that by proper adjustment of the 10<sup>23</sup> force constants any desired temperature dependence of the quantities dependent upon the thermal motion could be obtained. However, upon closer examination, one finds that there are certain restrictions on the temperature dependence of these quantities which are a direct result of the assumption that temperature-independent interatomic forces are harmonic. One example of these restrictions is the Dulong and Petit law for specific heats, which allowed early investigators to recognize the importance of the anharmonic terms at high temperature.

At low temperature the experimental specific heat of a material can be interpreted in terms of a completely harmonic model, which is consistent with the expected disappearance of anharmonicity at low temperature.

However, this gives no information on the harmonicity of the majority of the vibrational modes since the low-temperature specific heat is affected by only the low-frequency, long-wavelength vibrational modes.

The MSD and MSV on the other hand are dependent on all the vibrational modes, even at the lowest temperature. Hence a temperature study of these quantities could give information on the harmonicity of all the vibrational modes. In order to examine the harmonicity, it is necessary to know some of the restrictions on the MSD and MSV for a harmonic crystal.

Two of these restrictions are analogous to the Dulong-Petit law for specific heats. At high temperature for the *i*th particle in the *α* direction,

$$\langle V^2_{i\alpha} \rangle_T = \frac{kT}{m_i} \left[ 1 + \frac{K_{ii}^{\alpha\alpha}}{12m_i} \left( \frac{\hbar}{kT} \right)^2 + \dots \right] \quad (1)$$

and

$$\langle X^2_{i\alpha} \rangle_T = kT \left[ \frac{1}{K} + \frac{1}{12m_i} \left( \frac{\hbar}{kT} \right)^2 + \dots \right], \quad (2)$$

where *m<sub>i</sub>* is the mass of the *i*th atom and *K<sub>ii</sub><sup>αα</sup>* is the force constant for the *i*th atom in the *α* direction, for displacement of the *i*th atom in the *α* direction while all the other atoms in the crystal are fixed at their equilibrium positions.<sup>1</sup> *K*, which has dimensions of a force constant, is a complicated function of the microscopic force constants, independent of the masses of the atoms in the crystal.<sup>2</sup> At high temperature, both the MSD and the MSV are linear in the temperature.

In addition to these requirements on the classical behavior of the MSD and MSV, certain inequalities can be established among the classical and low-temperature limits of these quantities.<sup>1</sup> Of particular interest in this paper is the inequality which establishes the maximum low-temperature MSD for a given MSD at high temperature. This maximum MSD or minimum recoil-free fraction, at low temperature is given by an Einstein-model fit to the classical region. Housley and Hess<sup>1</sup> established, by further consideration of this inequality and the temperature dependence of the MSD, that if

\* This work supported in part by the National Aeronautics and Space Administration under Grant No. NsG484.

† Present address: Advanced Materials Research and Development Laboratory, Pratt and Whitney Aircraft, Middletown, Conn. 06458.

<sup>1</sup> R. M. Housley and F. Hess, Phys. Rev. **146**, 517 (1966).

<sup>2</sup> A. A. Maradudin and P. A. Flinn, Phys. Rev. **126**, 2059 (1962).

one knows the MSD at any temperature  $T$ , then a plot of the MSD versus temperature must lie between two straight lines which intersect at the particular  $T$ . One of these lines passes through the origin and the other has a zero-temperature intercept at the value

$$\langle X^2_{i\alpha} \rangle_0 = \frac{1}{2} \hbar (\langle X^2_{i\alpha} \rangle_T / m_i k T)^{1/2}. \quad (3)$$

We find that the experimental MSD and MSV for  $\text{Fe}^{++}$  in  $\text{FeCl}_2$  exceed these harmonic limits. The experimental behavior clearly indicates that the force constants have a substantial degree of anharmonicity, even at helium temperatures.

## II. EXPERIMENTAL METHOD

### A. Equipment

The absorption-velocity spectra were measured using an absorber of ferrous chloride mounted in a cryostat and a source of  $\text{Co}^{57}$  dissolved in a copper foil. The source was mounted to an electromechanical transducer and velocity sensor consisting of a mechanically coupled speaker pair. The velocity was controlled by means of an electrical feedback system such that the source spent nearly equal times at equal velocity interval. The number of transmitted gamma rays in each velocity interval was recorded in the analog mode of a multi-channel analyzer, with a random pulse generator used to record in the second half of the memory the time spent in each velocity interval.

In order to hold the sample for several days at any temperature between helium temperature and room temperature, a transmission helium cryostat was constructed.<sup>3</sup> By means of an electrothermal feedback system and a variable heat link between the sample mount and the liquid reservoir,<sup>4</sup> the temperature of the sample could be held for several days within 0.2°K of any desired temperature. With this spectrometer and cryostat the instrumental broadening is less than 0.003 mm/sec.

### B. Absorber Preparation

The samples studied in this work consisted of two unenriched powdered absorbers of anhydrous ferrous chloride. Since  $\text{FeCl}_2$  is very deliquescent, special care was taken to prevent water vapor from coming into contact with the powder. After the mounting procedure, the amount of hydration which occurred was checked by chemical analysis of similar samples and examination of the Mössbauer spectra.

The absorbers were prepared by first grinding the  $\text{FeCl}_2$  in an atmosphere of dry nitrogen. After dispersing the ferrous powder in toluene and allowing the larger particles to gravitate out of the toluene, the remaining ferrous material was allowed to settle into a lucite

container. The toluene was then removed by means of a liquid nitrogen trap, after which the container was closed, weighed to determine the thickness of the powder, and sealed with polystyrene cement.

The thickness uniformity was checked by measuring the transmission of 14-keV gamma radiation through many different regions on each absorber. As indicated by these measurements, the long-range variation in the thickness of these ferrous chloride absorbers was less than 1%.

In order to estimate the short-range variation in thickness of these absorbers, the absorber designated  $\text{FeCl}_2$ -2 was taken apart after the temperature study and examined under a microscope. The average variation in thickness due to the granular nature of the powder was less than  $\pm 7 \mu$ . This variation introduces an uncertainty in the recoil free fraction of less than  $\frac{1}{2}\%$ . A detailed discussion of the effects of granular absorbers is given in Ref. 5.

The average thickness of  $\text{Fe}^{57}$  in the absorber designated  $\text{FeCl}_2$ -1 was 0.570 mg/cm<sup>2</sup> and the thickness of  $\text{Fe}^{57}$  in the absorber designated  $\text{FeCl}_2$ -2 was 0.272 mg/cm<sup>2</sup>. The natural relative abundance of  $\text{Fe}^{57}$  is taken to be 0.0219.<sup>6</sup>

### C. Source Preparation

The principal radioactive source used in the measurements consisted of 3.0 mCi of  $\text{Co}^{57}$  dissolved in a thin copper foil. This source was prepared by drying approximately 3.5 mCi of  $\text{Co}^{57} \text{Cl}_2 \cdot 6\text{H}_2\text{O}$  solution on the surface of a copper foil which was then heated to 920–950°C for 1 h in a purified hydrogen atmosphere. After cleaning the surface, 3.0 mCi remained in the sample.

As a check on the source and as a calibration, the copper source was run against a natural iron absorber. The thickness-corrected experimental linewidth was found to be  $0.203 \pm 0.003$  mm/sec. Measurements on a less active copper source gave a corrected spectrum linewidth of  $0.196 \pm 0.003$  mm/sec, indicating that the 3.0-mCi source linewidth may be slightly greater than natural width. The linewidth of the 3.0-mCi source is assumed to be 0.105 mm/sec. The velocity separation of the hyperfine spectrum of iron as measured by Preston, Hanna, and Heberle<sup>7</sup> was used for a velocity calibration of the spectrometer.

### D. Background Correction

In addition to the 14-keV  $\gamma$  ray resulting from the direct nuclear decay, there are many other photons striking the NaI crystal. The highest intensity radiation comes from the 136-keV nuclear level. Most of these

<sup>3</sup> D. P. Johnson, G. A. Erickson, and J. G. Dash, *Rev. Sci. Instr.* **39**, 420 (1968).

<sup>4</sup> J. G. Dash and J. D. Siegwarth, *Rev. Sci. Instr.* **34**, 1276 (1963).

<sup>5</sup> J. D. Bowman, E. Kankleit, and B. Persson, *Nucl. Instr. Methods* **50**, 13 (1967).

<sup>6</sup> A. H. Wapstra, *J. Inorg. Nucl. Chem.* **3**, 329 (1957).

<sup>7</sup> R. S. Preston, S. S. Hanna, and J. Heberle, *Phys. Rev.* **128**, 2207 (1962).

photons can be distinguished from the 14-keV  $\gamma$  ray in the detector by pulse-height analysis. However, some of these photons are only partially absorbed in the thin crystal and appear to the detector as a 14-keV photon. This background fraction is determined by use of a 0.005-in. brass filter. This brass filter absorbs nearly all the photons below 14 keV and only 4% of the high-energy  $\gamma$  rays.<sup>8</sup> Thus, by measuring the count rate with and without the brass filter, the background fraction can be determined.

In addition to these high-energy  $\gamma$  rays, there are also many 6-keV x rays resulting from the  $K$  capture in the decay of the  $\text{Co}^{57}$  and from internal conversion in the iron. There also are x rays from the other materials in the source, absorber, and surroundings due to the photoelectric effect with the high-energy radiation. Fortunately, most of the materials used in this experiment are of sufficiently low  $Z$  so that these x rays are below the 14-keV pulse-height "window."

The above are the major contributions to the  $\gamma$ -ray spectrum. However, other inelastic scattering processes in the source and surrounding material can contribute to the nonresonant fraction, reducing the sharp fraction of photons below the inherent  $f$  of the source.<sup>8</sup> In source  $f$  measurements, these effects can be important since one is interested in determining the inherent  $f$  of the source. In absorber  $f'$  measurements, one simply need determine the sharp fraction of photons falling on the absorber in order to determine the resonant cross section of the absorber.

There may be, however, some small-angle inelastic scattering in the  $\text{FeCl}_2$  absorber or absorber mount which could change the effective sharp fraction incident on the absorber from that measured in a standard black absorber configuration.<sup>9</sup> When an absorber is first studied at room temperature and then mounted in a cryostat, there could be an additional modification of this fraction due to scattering from the changed environment or small-angle scattering in the beryllium windows and thermal-radiation shields.<sup>10</sup>

To check whether these considerations are important, the sharp fraction which exits from the cryostat after passing through an  $\text{FeCl}_2$  absorber, windows, and radiation shields was measured with a black absorber and compared with that measured in a standard black absorber configuration. The sharp fraction of the Cu source in both cases had a magnitude of  $0.703 \pm 0.003$  at 297°K, indicating no significant change in the sharp fraction resulting from the change in environment or small-angle scattering in the  $\text{FeCl}_2$  absorber. This value is slightly lower than the recoil-free fraction for copper reported by other authors. Housley, Dash, and Nuss-

baum<sup>11</sup> and Sprague<sup>12</sup> reported at 297°K an  $f$  of  $0.710 \pm 0.015$  and  $0.709 \pm 0.002$ , respectively. Steyert and Taylor<sup>10</sup> reported an  $f$  of  $0.727 \pm 0.015$  at 293°K.

### III. DISCUSSION AND RESULTS

#### A. Line Shape

The general shape, splitting, and linewidth of the Mössbauer spectrum are strong indications of the chemical environment in which the iron ions find themselves. Slight variations in the electric-field gradient or the number or type of electrons associated with the iron ion will produce a distortion and broadening of the Mössbauer spectrum. For example, adding one  $3d$  electron will change the shift by 0.8 mm/sec<sup>13</sup> or in terms of our experimental sensitivity, a variation of 0.01 of an electron would produce a perceptible line broadening. The experimental linewidth of the  $\text{FeCl}_2$  absorbers are within 10% of that predicted for a natural width absorber and source, except at the lowest temperature.

Figure 1 is a plot of the velocity spectrum of a ferrous-chloride absorber at 296.8°K. The presence of the two small minima outside the two main minima is due to a few percent of the ferrous chloride being in the monohydrate state, which is identified by its quadrupole splitting.<sup>14-17</sup> Based on the measured  $f'$  of  $\text{FeCl}_2 \cdot 4\text{H}_2\text{O}$ ,<sup>18</sup>

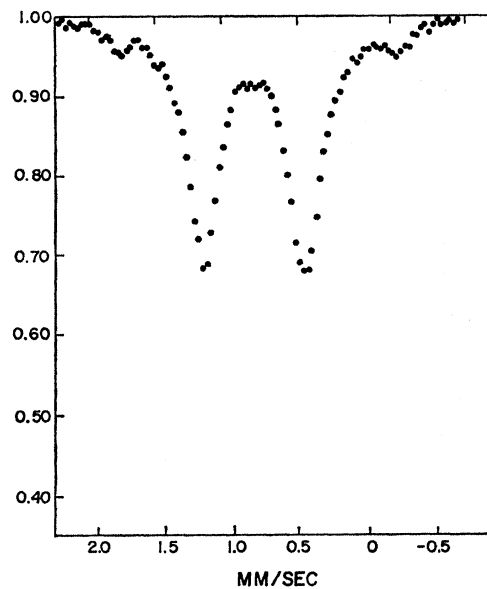


FIG. 1. Velocity spectrum of  $\text{FeCl}_2$  at room temperature.

<sup>11</sup> R. M. Housley, J. G. Dash, and R. H. Nussbaum, *Phys. Rev.* **136**, A464 (1964).

<sup>12</sup> D. L. Sprague, Ph.D. thesis, University of Washington, 1967 (unpublished).

<sup>13</sup> L. R. Walker, G. K. Wertheim, and V. Jaccarino, *Phys. Rev. Letters* **6**, 98 (1961).

<sup>14</sup> J. W. Hurley, R. C. Axtmann, and Y. Hazony, *Bull. Am. Phys. Soc.* **12**, 654 (1967).

<sup>15</sup> S. Chanda and G. R. Hoy, *Phys. Letters* **22**, 254 (1966).

<sup>16</sup> P. Zory, *Phys. Rev.* **140**, 1401 (1965).

<sup>17</sup> L. G. Lang, S. Benedetti, and R. L. Ingalls, *J. Phys. Soc. Japan* **17**, Suppl. B-1, 131 (1962).

<sup>18</sup> W. Kerler, *Z. Physik* **167**, 194 (1962).

<sup>8</sup> R. M. Housley, *Nucl. Instr. Methods* **35**, 77 (1965).

<sup>9</sup> R. M. Housley, N. E. Erickson, and J. G. Dash, *Nucl. Instr. Methods* **27**, 29 (1964).

<sup>10</sup> Discrepancies between  $f$  results, in and out of a cryostat, are attributed to this type of scattering by W. A. Steyert and R. D. Taylor, *Phys. Rev.* **134**, A716 (1964).

and our preliminary value for  $\text{FeCl}_2$ , the  $f'$  of this monohydrate state was estimated to be 0.30. Assuming this  $f'$ , then the percentage of iron in the anhydrous state can be determined from the area of these lines.

We have several cross checks on the calculated  $f'$  of the monohydrate. This value of  $f'$  is used for both  $\text{FeCl}_2$ -1 and  $\text{FeCl}_2$ -2 absorbers which have different percentages of monohydrate, and the above procedure yields consistent values for the  $f'$  of the anhydrous ferrous chloride. A stronger check is afforded by the area of the satellite lines at two temperatures in the classical region. Each measurement yields the product  $x_m f'$ , where  $x_m$  is the thickness of the monohydrate. Since the temperature dependence of the  $f'$  is known to be linear in  $T$ , the  $x_m$  and the  $f'$  are determined from these two measurements. This method gives an  $f'$  for the monohydrate which is consistent with the previously assumed value. The residual uncertainty in the recoil-free fraction of anhydrous  $\text{FeCl}_2$ , due to the contamination of monohydrate, is estimated to be less than 1%.

Figure 2 is a plot of the  $\text{FeCl}_2$ -2 velocity spectrum at nitrogen temperature, just above the Néel temperature at 27.7°K, and below the Néel temperature at 12.5°K. In agreement with Ôno, Ito, and Fujita,<sup>19</sup> we observe no hyperfine splitting below the Néel temperature,  $T_N = 23.6^\circ\text{K}$ . However, we do observe a large increase in linewidth. This increase in width is not symmetrical;

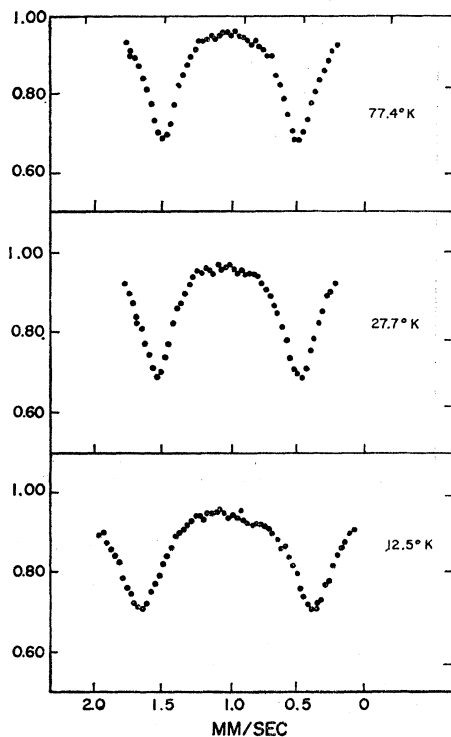


FIG. 2. Velocity spectrum of  $\text{FeCl}_2$  at 77.4, 27.7, and 12.5°K.

<sup>19</sup> K. Ôno, A. Ito, and T. Fujita, *J. Phys. Soc. Japan* **19**, 2119 (1964).

the width of one quadrupole-component line increasing by approximately 55% more than the width of the other component. As indicated by the single-crystal spectrum, the broader line is associated with the transition from the  $m_z = \frac{3}{2}$  level, which in the presence of a small magnetic field would broaden more than the  $m_z = \frac{1}{2}$  transition. Assuming that the broadening is due to a magnetic field, we arrive at an absolute value for the internal magnetic field of  $(4.5 \pm 1)$  kOe, in agreement with Ôno, Ito, and Fujita's results of  $(0 \pm 8)$  kOe.<sup>19</sup>

This result does not significantly modify these authors' explanation of the surprisingly small internal field below the Néel temperature. Their explanation is in terms of a near cancellation of the orbital, contact, and dipole contribution to the magnetic field at the nucleus. The results of Ôno *et al.*, which are consistent

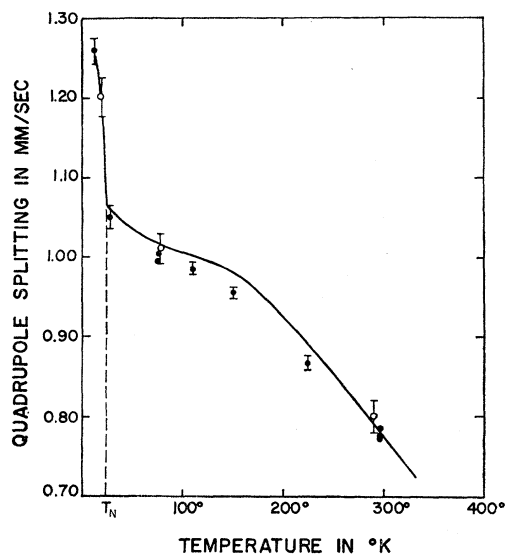


FIG. 3. Quadrupole splitting of  $\text{FeCl}_2$ . The solid circles are the results of this experiment. The open circles are the results of Ôno *et al.* (Ref. 19). The solid line is the theoretical curve of Ôno *et al.* for their empirical parameters.

with a magnetic field of exactly zero, have led to some speculation that the absence of a magnetic field is due to a rapid relaxation between the different magnetic states. However, our detection of a finite broadening supports the contention of Ôno *et al.* that there is a small finite field resulting from near cancellation of large terms. Figure 3 shows the quadrupole splitting of  $\text{FeCl}_2$  as a function of temperature, and is in good agreement with previous measurements.<sup>19</sup>

### B. Velocity Shift

As is well known, the velocity shift is made up of two physically distinguishable phenomena which are designated as the chemical shift and the thermal shift. The chemical shift, which results from an electrostatic interaction between the electrons and the nuclear

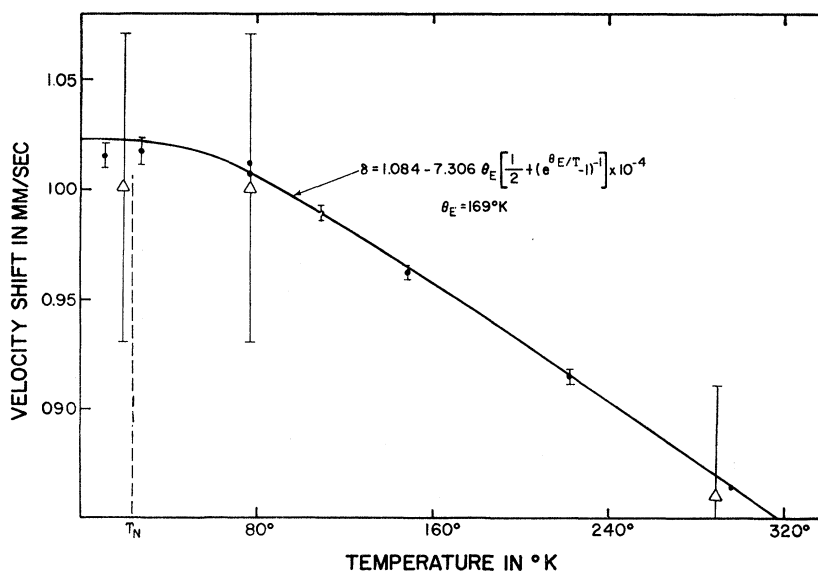


FIG. 4. The velocity shift of  $\text{FeCl}_2$ . The circles are our data for  $\text{FeCl}_2$ -1 and  $\text{FeCl}_2$ -2. The triangles are the data of Ono *et al.* (Ref. 19).

charge, is usually considered to be only weakly dependent upon temperature except possibly at phase transitions.<sup>7,20,21</sup> Assuming that the chemical shift is independent of the temperature, it can be included with the constant thermal shift of the  $\text{Fe}^{57}$  in the copper source as a temperature-independent parameter  $\delta_0$ . The total shift can then be written as

$$\delta = \delta_0 - \langle V^2 \rangle_T / 2c, \quad (4)$$

where

$$\langle V^2 \rangle_T = \sum_{\alpha=1}^3 \langle V^2_{\alpha} \rangle_T.$$

In Fig. 4, the temperature dependence of the velocity shift of the ferrous-chloride absorbers versus a room-temperature copper source is denoted. The solid line represents a theoretical fit to the high-temperature data with  $\delta_0 = (1.084 \pm 0.002)$  mm/sec and a thermal shift given by a characteristic Einstein temperature of  $(169 \pm 5)^{\circ}\text{K}$ . This temperature dependence corresponds to that in Eq. (1), with

$$K_{ii} = \frac{1}{3} \sum_{\alpha=1}^3 K_{ii}^{\alpha\alpha} = (0.46 \pm 0.02) \text{ mdyn}/\text{\AA}.$$

At low temperature, the velocity shift falls below that predicted by any harmonic model for the frequency spectrum and a temperature-independent chemical shift. However, because of the antiferromagnetic transition at  $23.6^{\circ}\text{K}$  this data alone cannot be used to establish the origin of this deviation.

### C. Mössbauer Fraction

The area of the absorption spectrum was used to determine the resonant cross section of these absorbers.

<sup>20</sup> R. V. Pound, G. B. Benedek, and R. Drever, *Phys. Rev. Letters* **7**, 405 (1961).

<sup>21</sup> R. Ingalls, *Phys. Rev.* **155**, 157 (1967).

This procedure is particularly useful because the area is independent of the source line shape and velocity-independent instrumental broadening and is sensitive enough to allow the use of relatively thin absorbers, in which case the area is only very weakly dependent upon the absorber line shape.

In the case of a thin absorber, the area can be expressed as a simple product of the  $f$  of the source and the  $f'$  of the absorber, independent of the source or absorber line shape. However, for thicker absorbers, the area is no longer linear in  $f'$  and this saturation depends upon the line shape of the absorber. The effect of a small broadening of the absorber line due to microscopic variations in the environment can be estimated if one assumes that the absorber line shape is given by a broadened but still Lorentzian line of width  $\Gamma$ . In this case the area is given by an expression similar to that for a natural width absorber evaluated by Born:<sup>22,22a</sup>

$$A = \pi f \Gamma Z e^{-t} [I_0(Z) + I_1(Z)], \quad (5)$$

where  $I_n(Z)$  is a hyperbolic Bessel function of order  $n$  and  $Z = f' n_a \sigma_0 \Gamma_0 / 2\Gamma$ .  $n_a$  is the number density of  $\text{Fe}^{57}$  atoms in the absorber,  $\sigma_0 = 2.35 \times 10^{-18} \text{ cm}^2$  is the maximum nuclear cross section,<sup>23</sup>  $\Gamma_0 = 4.65 \times 10^{-12} \text{ keV}$  or  $0.097 \text{ mm/sec}$  is the full width at half-maximum,<sup>24</sup> and  $t$  is the thickness of the absorber. The effect of the broadening is shown in Fig. 5.  $\Gamma$  can be determined from

<sup>22</sup> M. Born, *Optik* (Julius Springer-Verlag, Berlin, 1933).

<sup>22a</sup> Note added in proof. This expression neglects the polarization dependence of the nuclear-absorption cross section. The MSD in Fig. 6 will be reduced by  $(0.06 \pm 0.01) \times 10^{-2} \text{ \AA}^2$  if the polarization effects are included. See R. M. Housley, U. Gonser, and R. W. Grant, *Phys. Rev. Letters* **20**, 1279 (1968).

<sup>23</sup> R. H. Nussbaum and R. M. Housley, *Nucl. Phys.* **68**, 145 (1965).

<sup>24</sup> A. H. Muir, K. J. Ando, and H. M. Coogan, *Mössbauer Effect Data Index, 1958-1965* (Interscience Publishers, Inc., New York, 1966).

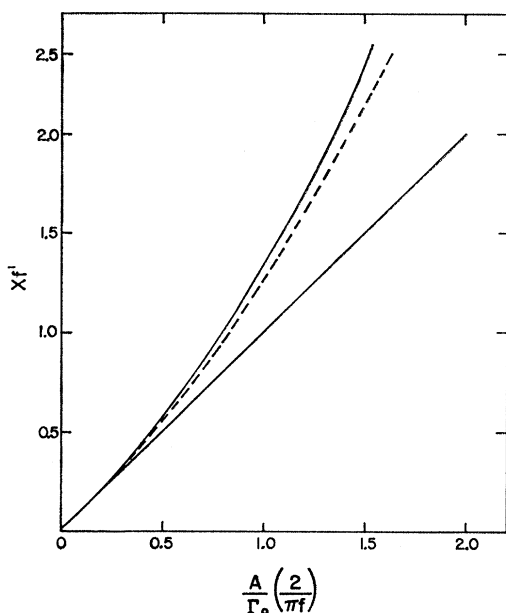


FIG. 5. Plots of the thickness of the absorber for various absorption-line widths as a function of the experimental area. The upper curve corresponds to an absorption line of natural width. The dotted line corresponds to an absorption line which is 20% broader than natural width. The lower curve corresponds to an absorption line of infinite linewidth.

the velocity spectrum by using an expression given by O'Connor.<sup>25</sup>

In ferrous chloride, the absorber spectrum is split into two lines due to an electric field gradient at the nucleus, necessitating a slight modification of the preceding area to thickness relations. When the quadrupole splitting is large, corresponding to no overlap, the area of each line can be measured separately and Eq. (5) can be used with  $Z_1 = \frac{1}{4}(x f_{3/2})$  and  $Z_2 = \frac{1}{4}(x f_{1/2})$ , where  $x = n_a \sigma_0 \Gamma_0 / \Gamma$ .  $f_{3/2}$  and  $f_{1/2}$  will be related to the  $f'$  of the material and the orientation of the crystals. The effect of the small overlap between these two peaks can be estimated by using an approximate expression of Bykov and Hien.<sup>26</sup> On this basis, the error introduced by ignoring the slight overlap is found to be less than 0.2%.

The asymmetry in the observed spectrum ( $f_{3/2} \neq f_{1/2}$ ) could be caused by either the Karyagin effect<sup>27</sup> or a preferred orientation of the small grains in the powdered absorber. The latter can be eliminated as a possible determinant because the asymmetry is independent of the absorber orientation.

In the case of axial symmetry and harmonic interatomic forces, the Karyagin effect<sup>27</sup> can be used to determine the angular dependence of the MSD of the ferrous ion from randomly oriented powder-absorber

data. For threefold axial symmetry as exists in  $\text{FeCl}_2$ ,

$$f'(\theta, \varphi) = e^{-\langle X^2(\theta, \varphi) \rangle_T / \lambda^2}, \quad (6)$$

where

$$\langle X^2(\theta, \varphi) \rangle_T = c^2(T) \cos^2\theta + a^2(T) \sin^2\theta, \quad (7)$$

$\lambda$  is the reduced wave length of the 14-keV radiation,  $c^2(T)$  is the MSD parallel to the symmetry axis, and  $a^2(T)$  is the MSD perpendicular to the axis.<sup>28</sup> The probability of recoilless absorption or emission is given by the product of the transition probability and the recoil-free fraction, i.e.,

$$f_{3/2}(\theta) = \frac{3}{4} f'(\theta) (1 + \cos^2\theta) \quad (8)$$

and

$$f_{1/2}(\theta) = \frac{1}{4} f'(\theta) (5 - 3 \cos^2\theta). \quad (9)$$

For randomly oriented powdered absorbers,

$$f_{3/2} = \frac{3}{8} \int_0^\pi f'(\theta) (1 + \cos^2\theta) \sin\theta \, d\theta \quad (10)$$

and

$$f_{1/2} = \frac{1}{8} \int_0^\pi f'(\theta) (5 - 3 \cos^2\theta) \sin\theta \, d\theta. \quad (11)$$

Based on Eqs. (10) and (11) and the measured  $f_{3/2}$

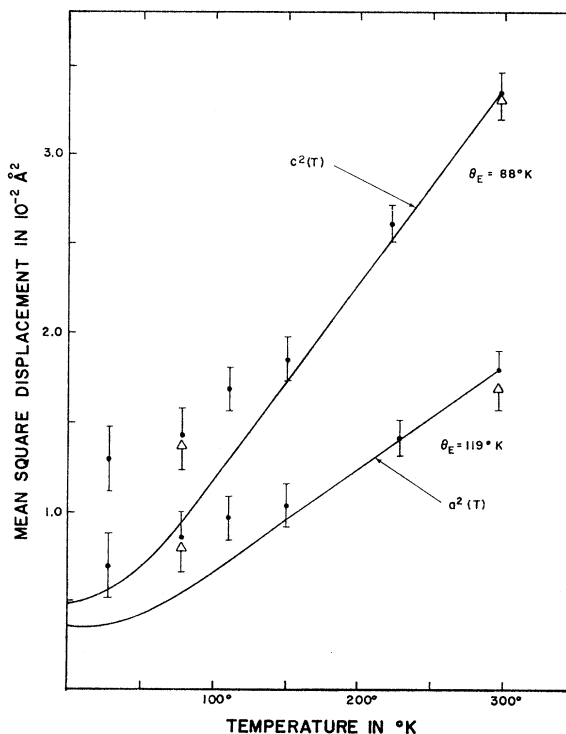


FIG. 6. Mean square displacement ( $-\lambda^2 \ln f$ ) of the ferrous ion parallel ( $c^2$ ) and perpendicular ( $a^2$ ) to the  $c$  axis of ferrous chloride. The circles correspond to  $\text{FeCl}_2\text{-2}$  and the triangles correspond to  $\text{FeCl}_2\text{-1}$ . The solid lines are curves based on the Einstein model of the frequency distribution.

<sup>25</sup> D. A. O'Connor, Nucl. Instr. Methods 21,318 (1963).

<sup>26</sup> G. A. Bykov and P. Z. Hein, Zh. Eksperim. i Teor. Fiz. 43, 909 (1962) [English transl.: Soviet Phys.—JETP 16, 646 (1963)].

<sup>27</sup> S. V. Karyagin, Dokl. Akad. Nauk. SSSR 148, 1102 (1963) [English transl.: Proc. Acad. Sci. USSR, Phys. Chem. Sect. 148, 110 (1964)].

<sup>28</sup> D. P. Johnson, Ph.D. thesis, University of Washington, 1967 (unpublished).

and  $f_{1/2}$ , the MSD of the ferrous ion parallel [ $c^2(T)$ ] and perpendicular [ $a^2(T)$ ] to the threefold symmetry axis is determined.

As can be seen in Fig. 6, the experimental MSD at low temperature is considerably larger than that predicted for an Einstein model. This excess MSD at low temperature, as discussed in the Introduction, cannot be described in terms of any temperature-independent distribution of harmonic modes. Because of the large deviation from harmonic behavior at low temperature, this is not the usual high-temperature anharmonicity, which is due to the higher order terms in the expansion becoming significant as the temperature increases, but is an anharmonicity which requires a large number of higher-order terms to specify the potential even at the lowest temperature. The effect of this "low-temperature anharmonicity" on the Debye-Waller factor is discussed in detail in Ref. 29.

#### IV. LOW-TEMPERATURE ANHARMONICITY IN $\text{FeCl}_2$ AND OTHER MATERIALS

The crystal structure of  $\text{FeCl}_2$  consists of hexagonal layers of chloride ions with hexagonal layers of ferrous ions between every two layers of chloride. The ferrous ions fit in the octahedral interstices of the nearly perfect close-packed array of chloride ions.<sup>30</sup> Assuming 0.74 and 1.81 Å for the cation and anion radii, respectively, the radius of the octahedral interstices is approximately 0.05 Å larger than the ferrous ion which suggests that the ferrous ion is relatively loosely bound in the octahedral cage of the six nearest-neighbor chloride ions.<sup>31</sup> This loose binding is also indicated by the small force constant found for the crystal. The stretching force constant in the molecule is<sup>32</sup> 2.23 mdyn/Å as compared to the 0.46 mdyn/Å found for  $K_{ii}$  in this Mössbauer study.<sup>33</sup>

The nearly close-packed array of the relatively large chloride ions and the weak force constant suggest that the size of the cage around the ferrous ion is not limited by the overlapping iron-chloride electron clouds but rather by chloride-chloride electron clouds overlapping. Thus, the ferrous ion nearest-neighbor force constants are not determined by the strong overlap forces alone but are strongly influenced by the electrostatic and covalent forces. The covalent forces will give an added attraction, which is not a linear function of the separation, and this will tend to drive the ferrous ion toward one of its chloride neighbors. The purely electrostatic effects will also tend to make the center of symmetry an unstable equilibrium position. Because of the short-

range nature of the overlap forces, the unstabilizing forces acting on the ferrous ion could dominate at the center of symmetry. Under these conditions there is no minimum at the center of symmetry, and the potential is lower at regions closer to the chloride ions.<sup>34</sup> If the energy barriers between these various minima are not much greater than the zero-point energy, the ferrous ion will not be trapped at any of these positions and the dynamic center will still be at the center of symmetry. Accordingly, the ferrous ion will move in a very non-harmonic potential, especially at low temperatures, and the mean-square displacement will be larger at low temperatures than expected on the basis of a harmonic analysis of the high-temperature results.

An extreme example of this type of behavior is found in small ionic impurities in a larger lattice. For example, lithium impurities in potassium chloride and potassium bromide show a multiminimum potential.<sup>35-38</sup> In these cases the minima in the potential are large enough so that upon cooling to low temperatures these ions will actually settle into one of the off-center minima. Another example of this type of behavior is the growing class of displacive ferroelectric materials. Although the ferroelectric character comes from a collective phenomenon which forces all the displacive atoms to settle into equivalent sites, an essential feature of this phenomenon is the instability of the ion at the center of symmetry.<sup>39-41</sup>

It is not necessary for these unstabilizing forces to dominate in order to produce appreciable low-temperature anharmonicity. If the forces are nearly equal when the ferrous ion is at the center of symmetry, the ion may move in a very weak potential near the cell center, but in a stronger force field near the chloride ions.<sup>34</sup> An approximation which would show some of the features of this intermediate situation would be a square well. This type of potential was suggested by Steyert and Craig<sup>42</sup> for anomalous recoil free-fraction results found for Fe<sup>57</sup> impurities in indium.<sup>42,43</sup>

Based on a single-particle square well, comparison of the mean-square displacement and the mean-square

<sup>34</sup> An example of this type of potential is found in J. E. Lennard-Jones and A. F. Devonshire, Proc. Roy. Soc. (London) **163**, 53 (1937).

<sup>35</sup> G. Lombardo and R. O. Pohl, Phys. Rev. Letters **15**, 29 (1965).

<sup>36</sup> M. E. Baur and W. R. Salzman, Phys. Rev. Letters **16**, 701 (1966).

<sup>37</sup> F. C. Baumann, J. P. Harrison, R. O. Pohl, and W. D. Seward, Materials Science Center Report No. 630, Cornell University, 1967 (unpublished).

<sup>38</sup> J. A. D. Matthew, Materials Science Center Report No. 373, Cornell University, 1965 (unpublished).

<sup>39</sup> W. Cochran, Advan. Phys. **9**, 387 (1960).

<sup>40</sup> A. Chen and F. Chernov, Phys. Rev. **154**, 493 (1967).

<sup>41</sup> J. C. Slater, Phys. Rev. **78**, 748 (1950).

<sup>42</sup> W. A. Steyert and P. P. Craig, Phys. Letters **2**, 165 (1962); P. P. Craig, R. D. Taylor, and D. E. Nagle, Nuovo Cimento **22**, 402 (1961).

<sup>43</sup> Currently there is some dispute over these results; see P. A. Flinn, V. Gonser, R. W. Grant, and R. M. Housley, Phys. Rev. **157**, 538 (1967).

<sup>29</sup> J. G. Dash, D. P. Johnson, and W. M. Visscher, Phys. Rev. **168**, 1087 (1968).

<sup>30</sup> R. O. MacLaren and N. W. Gregory, J. Am. Chem. Soc. **81**, 2649 (1959).

<sup>31</sup> M. K. Wilkinson, J. W. Cable, E. O. Wollan, and W. C. Koehler, Phys. Rev. **113**, 497 (1959).

<sup>32</sup> G. E. Loroi, J. Chem. Phys. **36**, 2879 (1963).

<sup>33</sup> D. P. Johnson and J. G. Dash, Bull. Am. Phys. Soc. **12**, 378 (1967).

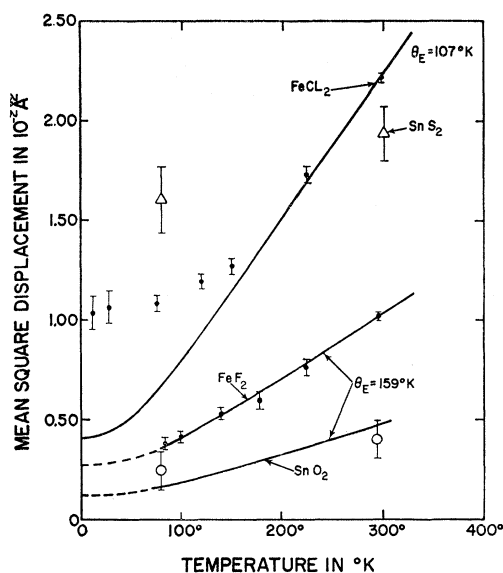


FIG. 7. The mean square displacements of various compounds. These mean square displacements are based on the assumption that the crystals are harmonic. The solid circles are the results of our experiments on  $\text{FeF}_2$  and  $\text{FeCl}_2$ . The open circles are the results of Hien *et al.* (Ref. 45) and Shapiro *et al.* (Ref. 46) for  $\text{SnO}_2$ . The triangles are the results of Bryukhanov *et al.* for  $\text{SnS}_2$  (Ref. 47). The solid lines are curves based on the Einstein model of the frequency distribution.

velocity indicates that the potential has a region of negative force constant resulting in a multiminimum potential. However, the effects of the collective modes are very hard to estimate and they would tend to reduce this difference between the square well and the experimental results.

Dash, Johnson, and Visscher<sup>29</sup> examined the effect of low-temperature anharmonicity on the Debye-Waller factor in the high and low temperature limit for various simple models for the interatomic potentials. A salient feature of the potential wells used to characterize the low-temperature anharmonicity is a central region of vanishing force constant. The effect of varying the range of the flat region and the hardness of the walls, and the effect of coupling this anharmonic potential to a harmonic system are considered. In the classical limit and under certain simplifying assumptions in the low-temperature limit, they found that the  $f$ -factor can be expressed as a product of harmonic and anharmonic terms. On this basis, the radius of the "flat region" for  $\text{Fe}^{++}$  in  $\text{FeCl}_2$  is estimated to be  $(0.07 \pm 0.02) \text{ \AA}$ .

Since the large difference in size between the positive and negative ions is an essential part of this model, a reduction in the size differences should reduce this anharmonicity. Thus ferrous fluoride, which is made up of negative fluoride ions which are 25% smaller than the

negative chloride ions, should show a greatly reduced anharmonicity. In this case the ferrous ions will not fit in a hole between different hexagonal layers of fluoride ions. Hence the crystal distorts from the calcium chloride to a cassiterite ( $\text{SnO}_2$ ) structure. In this case the separation is not determined by the fluoride-fluoride electron cloud overlap forces but by the iron-fluoride electron-overlap forces. In this system the fluoride ions collapse around the ferrous ion due to the attractive forces until the repulsive-overlap forces dominate. Therefore, we would expect no low-temperature anharmonicity for  $\text{FeF}_2$ . The experimental behavior of the  $f$  factor for Fe in  $\text{FeF}_2$  agrees with this prediction<sup>44</sup> and this behavior is shown in Fig. 7.

Since the structure of ferrous fluoride is the same as that of  $\text{SnO}_2$ , we reexamined previous Mössbauer results for  $\text{Sn}^{119}$  in this material.<sup>45,46</sup> The rather limited results are also shown in Fig. 7 and they can also be fitted by a strictly harmonic analysis. The  $\text{SnS}_2$ , on the other hand, has relative ion sizes even more disparate than the  $\text{FeCl}_2$ , with a crystal structure closely related to that of ferrous chloride. The only difference is a slightly modified stacking of the hexagonal sulfide planes, with the  $\text{Sn}^{+4}$  ion loosely held in spaces between two sulfide planes. Figure 7 shows the results for  $\text{SnS}_2$  at nitrogen and room temperatures.<sup>47</sup> These data indicate that the Sn ion in  $\text{SnS}_2$  is in an even more anharmonic potential than the Fe ion in  $\text{FeCl}_2$ , which is consistent with the larger disparities in ionic sizes.

In addition to these Mössbauer studies, anomalous low-temperature behavior has been recently observed in several high-temperature superconductors<sup>48-50</sup> which can also be attributed to a low-temperature anharmonicity. Thus, the widely accepted view that the interatomic potentials can be approximated by one or two terms of a Taylor-series expansion at low temperatures may not be correct, not only for the well-known case of light van der Waals solids,<sup>51</sup> but also in high-temperature superconductors, small ionic and metallic impurities, and for pure materials consisting of atoms with large size differences.

<sup>44</sup> D. P. Johnson and J. G. Dash, *Bull. Am. Phys. Soc.* **12**, 901 (1967).

<sup>45</sup> P. Z. Hien and V. S. Shpinel, *Zh. Eksperim. i Teor. Fiz.* **44**, 393 (1963) [English transl.: *Soviet Phys.—JETP* **17**, 268 (1963)].

<sup>46</sup> V. G. Shapiro and V. S. Shpinel, *Zh. Eksperim. i Teor. Fiz.* **46**, 1960 (1964) [English transl.: *Soviet Phys.—JETP* **19**, 1321 (1964)].

<sup>47</sup> V. A. Bryukhanov, N. N. Delyagin, A. A. Opalenko, and V. S. Shpinel, *Zh. Eksperim. i Teor. Fiz.* **43**, 432 (1962) [English transl.: *Soviet Phys.—JETP* **16**, 310 (1963)].

<sup>48</sup> L. R. Testardi, R. R. Soden, E. S. Greiner, J. H. Wernick, and V. G. Chirba, *Phys. Rev.* **154**, 399 (1967).

<sup>49</sup> L. R. Testardi and T. B. Bateman, *Phys. Rev.* **154**, 402 (1967).

<sup>50</sup> J. S. Shier and R. D. Taylor, *Solid State Commun.* **5**, 147 (1967).

<sup>51</sup> G. L. Pollack, *Rev. Mod. Phys.* **36**, 748 (1964).